https://doi.org/10.5194/egusphere-2026-988
Preprint. Discussion started: 27 February 2026

Krill defecation at depth reduces carbon flux attenuation in the Weddell Sea euphotic zone.

Authors: Florence Atherden[1], Emily Rowlands[1], Gareth Flint[1], Sophie Fielding[1], Katrin Schmidt[2], Elaine Fileman[3], Angus Atkinson[3], Clara Manno[1]

1. British Antarctic Survey, Cambridge, UK
2. University of Plymouth, Plymouth, UK
3. Plymouth Marine Laboratory, Plymouth, UK

Corresponding authors: Florence Atherden, flrden19@bas.ac.uk, Clara Manno, clanno@bas.ac.uk

Short summary

The Southern Ocean influences global climate, in part, through biological production of carbon-rich particles which trap atmospheric carbon in the deep ocean. Our study highlights that krill migrating to 50-100 m and defecting carbon-rich pellets effectively counteracts the 'typical' scenario where the quantity of particles rapidly decreases from the surface, ultimately increasing how much atmospheric carbon is stored. These processes are of global benefit, but vulnerable in a changing climate.

Abstract

The Weddell Sea, Southern Ocean, is a highly productive location of deep-water formation and a globally important site of carbon sequestration. Here, the biological carbon pump is dominated by particulate processes (e.g. zooplankton faecal pellets and phytoplankton detritus). However, climate driven changes in sea ice have the potential to disrupt these processes, highlighting a need for contemporary observations. This study quantified the flux of particulate organic carbon (POC) and nitrogen (PON) across three depths (50, 100 ,150 m) at five locations (including shelf, off shelf, ice covered and ice-free environments) in the western Weddell Sea using a drifting sediment trap. POC and PON fluxes were greater on shelf than off-shelf, likely reflecting increased nutrient supply and productivity on shelf. No strong patterns between sea ice and ice-free stations were present, likely because the ice pack was constantly shifting, with most sites influenced by sea ice. The POC flux remained stable or increased with depth at most stations, ranging from 42.5 - 364.1 mg C m^{-2} day^{-1} (mean of 123.2 mg C m^{-2} day^{-1}). Krill faecal pellets represented 98% of all pellets, which contributed an estimated 17-99 % (median of 48 %) of the POC flux. The faecal pellet flux peaked at 100 m across the shelf, suggesting krill defecating at depth during daily migrations effectively counteracted attenuation in the upper ocean. Our findings emphasise the importance of zooplankton mediated processes in determining the particle flux and the benefits of resolving the vertical flux at a resolution which incorporates their ecology. It is unclear how changing sea ice dynamics will impact zooplankton, so a process-driven understanding of biogeochemical fluxes is integral for predicting the future of carbon cycling in the Southern Ocean.

Introduction

The Southern Ocean is a globally important site of carbon sequestration (DeVries, 2022). This is largely achieved by cool waters, deep water formation and a strong biological carbon pump (BCP), the process by which organisms mediate the transfer of carbon from surface waters into the deep ocean (Volk and Hoffert, 1985). In the Southern Ocean, most total organic carbon is

https://doi.org/10.5194/egusphere-2026-988
Preprint. Discussion started: 27 February 2026

produced as particulates rather than dissolved material (Carlson et al., 2000). These particulates consist of protists, detritus, aggregates and zooplankton faecal pellets, moults and carcasses etc (Alldredge and Silver, 1988; Turner, 2015). The euphotic zone determines the potential upper limit of the biological carbon pump through primary production; however, as these particles sink out of the euphotic zone, they are progressively modified (e.g. by fragmentation or aggregation), solubilised, remineralised and repackaged. This results in the flux attenuating with depth, often rapidly, as particulate organic carbon (POC) is converted into dissolved inorganic carbon (DIC) (Martin et al., 1987; Le Moigne, 2019; Volk and Hoffert, 1985). Though the particle flux can experience intense remineralisation in the upper ocean, ephemeral high production events or zooplankton driven modifications can prevent rapid attenuation with depth (Buesseler and Boyd, 2009). High production events may arise after the collapse of a bloom causing rapidly sinking pulse of particulates (Lacour et al., 2023; Manno et al., 2020) and zooplankton can significantly impact the flux through production of faecal pellets and detritivory. Faecal pellet production repackages material into dense, fast sinking particles, contributing to the flux (Cavan et al., 2015; Liszka et al., 2019; Manno et al., 2015). Conversely, detritivory and sloppy feeding can fragment particles, reducing their size and sinking rate, contributing to flux attenuation (Mayor et al., 2014). The balance of these processes is highly dependent upon the resident zooplankton community as well as the composition and bloom stage of the primary producers (Lacour et al., 2023; Le Moigne et al., 2015; Steinberg and Landry, 2017).

Within the Southern Ocean, the Weddell Sea is simultaneously highly productive and a site of deep-water formation, helping to drive the global thermohaline ocean circulation (Tally, 2013). Consequently, it is of global biogeochemical consequence. Indeed, the Weddell Sea accounts for ~ 25% of Southern Ocean productivity, averaging ~ 477 Tg C a^{-1} (Arrigo et al., 2008). However, this productivity is largely focused on the shelf and the marginal ice zone(Arrigo et al., 2008; El-Sayed and Taguchi, 1981). Iron and light availability typically limit productivity in the Southern Ocean. However, sea ice, ice shelf associated melt waters and shelf waters often contain elevated nutrient concentrations, helping to fuel phytoplankton blooms (Arrigo et al., 2008; Klunder et al., 2014; Middag et al., 2013; Smith and Nelson, 1985). This productivity supports a wealth of secondary consumers, including Antarctic krill (*Euphausia superba)* that directly impact the BCP via the production of dense, fast sinking faecal pellets (FPs), as well as rapid grazing rates exerting top-down pressures on phytoplankton blooms (Whitehouse et al., 2009). Although estimates of krill biomass from the Weddell Sea are scarce as the area is difficult to access (Atkinson et al., 2017), observed values range from 1-68 g m^{-2} wet weight in open water and 10-100 g m^{-2} under ice (Brierley et al., 2002; Daly and Macaulay, 1988; Guihen et al., 2014). Model based estimates of krill contributions to the BCP suggest the northern Weddell Sea marginal ice zone may be one of the most productive regions in the Southern Ocean, with a potential contribution of up to 325-3350 mg C m^{-2} day^{-1} in spring (Belcher et al., 2019). This high productivity coupled with its hydrography makes the Weddell Sea a site of global biogeochemical importance (Brown et al., 2015; Hoppema, 2004).

As a major contributor to deep water formation, the Weddell Sea generates up to 60% of Antarctic Bottom Water, the most voluminous and densest water mass on earth (Johnson, 2008; Orsi et al., 1999). Carbon sequestration periods can be increased when POC is remineralised in regions where deep water is formed (Baker et al., 2022), and as such these physical processes combined with the intense biological particulate production make carbon sequestration highly efficient in the Weddell Sea (Hoppema, 2004; Nissen et al., 2022; Volk and Hoffert, 1985). The Weddell Sea is experiencing rapid climate change, with a recent shift towards decreasing sea

https://doi.org/10.5194/egusphere-2026-988
Preprint. Discussion started: 27 February 2026

ice extent and thickness (Joshi et al., 2024). Warming, changes to sea ice and ice shelf melt dynamics have potential to impact both deep water formation and the resident plankton community, which in turn may impact the capacity of the Weddell Sea to act as a carbon sink (Nissen et al., 2022). Consequently, improving our understanding of the mechanisms regulating the magnitude of the carbon pump in the Weddell Sea shelf and marginal ice zone, including characterisation of the vertical carbon flux itself, is of vital importance.

This study quantifies and characterises the variability of daily vertical biogeochemical fluxes across 50, 100 and 150 m in the western Weddell Sea, using a custom-built drifting sediment trap (DST) (Rowlands et al., under review). The DST was deployed on and off the shelf, within sea ice and in open water. This study aims to characterise the major inputs into the biogeochemical particle flux, and how these change with the environment and across depths. Results provide insight on Southern Ocean carbon cycle drivers by capturing the flux both where the upper limit of carbon flux is 'set' and the greatest influence on attenuation is exerted (Buesseler et al., 2020).

Methods

Sampling deployments

The DST was deployed in five occasions from the *RSS Sir David Attenborough* in the Weddell Sea during February 2024, with each deployment lasting between 11.4 and 20.5 hours (Supplementary Table 1). The first deployment (S1) took place while sheltering from rough weather, consequently the DST remained tethered to the ship via a line (5 m from the ship) to prevent loss of the trap. Both the trap and the ship drifted ~ 1 km during deployment. Thereafter the trap was deployed freely drifting (Figure 1).

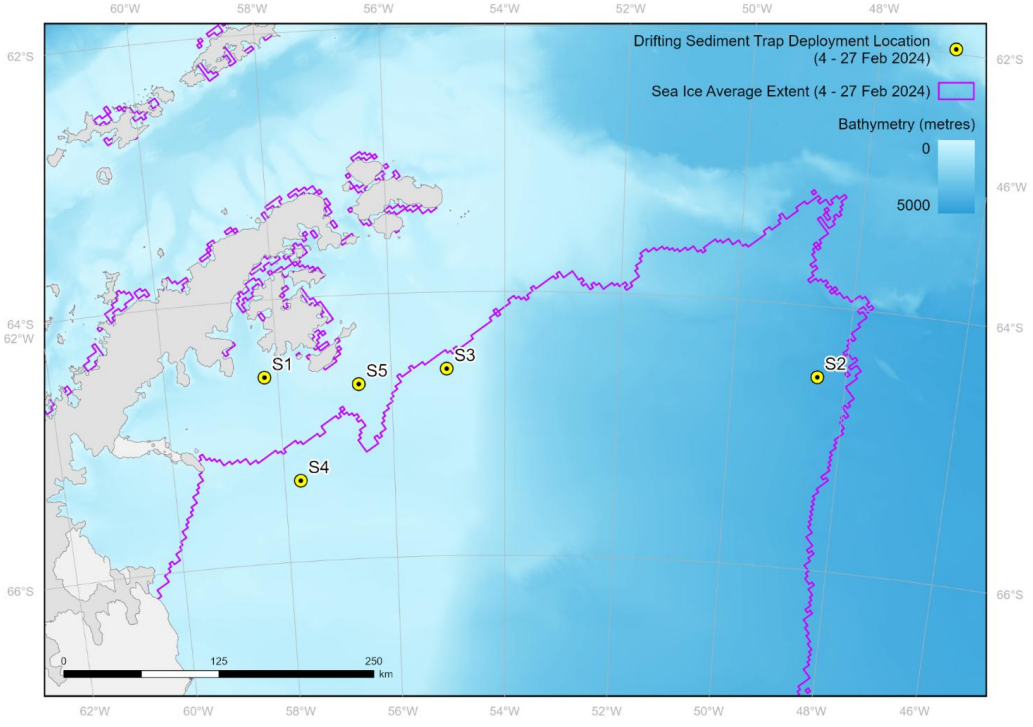

https://doi.org/10.5194/egusphere-2026-988
Preprint. Discussion started: 27 February 2026

Figure 1. Map of all five deployments across the Weddell Sea during February 2024 with the average sea ice extent (threshold of 15% sea ice concentration) for the entire sampling period in purple. Maps produced by Mapping and Geographic Information Centre, British Antarctic Survey, 2025.

A full description of the custom DST (developed in house at the British Antarctic Survey) is available from Rowlands et al., (submitted). In brief, the DST consists of a surface float fitted with an Iridium beacon, a vertical array of carousels (at 50, 100 and 150 m depth) with collection cannisters and a 10 kg weight at the bottom of the line. The three carousels are each fitted with steel, 6.2L collection canisters with an opening of 0.012 m^2. The DST is fitted with a messenger fired closing mechanism. At the end of the deployment, the messenger was released prior to recovery, closing the lids on the collection cannisters and preventing contamination which could result in an overestimation of the flux as the trap is hauled onboard. With each deployment a Conductivity-Temperature-Depth (CTD) profile was taken, equipped with the following instruments: a Sea-Bird SBE 9plus CTD system which included two Sea-Bird SBE3plus temperature sensors, Sea-Bird SBE4C conductivity sensors and a Paroscientific Digiquartz pressure sensor, a WETLabs Coloured Dissolved Organic Matter fluorometer and a SBE18 pH sensor (which replaced CDOM fluorometer from S3). Due to logistics, the closest CTD profile (-65.4087 N, -57.8138 E) to S4 (-65.3866 N, -57.7157 E) was 5.16 km away. The mixed layer depth (MLD) was identified by ascertaining the depth at which the density was equal to the density at 10 m + 0.3 kg m^3. Analysis and figure generation for CTD profile data was carried out in R (version 4.3.2).

On-ship sample preparation

Once recovered, the DST was processed immediately. Water was decanted from the DST carousel into 10L carboys (pre-rinsed three times with Milli-Q). The carousels were rinsed three times with Milli-Q water to ensure all particulates entered the carboys. Throughout, each carboy was gently but thoroughly stirred immediately prior to any subsampling to ensure representativeness. For particulate organic carbon (POC), particulate organic nitrogen (PON), 600 ml of water was filtered onto pre-combusted (450°C, 16 hrs), pre-weighed glass fibre filters (GF/F, 25 mm, 0.45 µm pore size, Whatmann) and rinsed with Milli-Q water (under < 20 mbar of vacuum pressure). Blanks were created by filtering 600 ml of Milli-Q water onto pre-combusted glass fibre filters as above. With the exception of S1 (where no replicates were taken), two replicates were taken from each depth and each deployment. All particulate samples were then air-dried for 24 hours in a fume hood and stored at -20°C until analysis at British Antarctic Survey, Cambridge, UK. To characterise the particles within the flux (e.g. faecal pellets, eggs), two 250 ml subsamples were taken per depth and deployment. These quantitative samples were then spiked with 13 ml of 37 % formaldehyde to reach a final concentration of 2% formalin.

Laboratory analyses

Elemental analyses

POC, PON and blank samples were fumed for 24 hours with 37 % HCl in a desiccator to remove the inorganic carbon content. POC and PON filters and filter blanks were placed in sterile nickel capsules, and analysed using a CE Instruments NA2500 elemental analyser, calibrated using an acetanilide calibration standard with a known % C and % N of 71.09 % and 10.36 % respectively. Standards were interspersed regularly between samples to measure and correct for drift with an analytical precision of ±0.3 %. Flux (mg m^{-2} day^{-1}) was calculated using the following equation (Eq. 1).

https://doi.org/10.5194/egusphere-2026-988
Preprint. Discussion started: 27 February 2026

$$(Eq.\,1) \qquad Flux\ (mg\ m^{-2} day^{-1}) = \frac{m}{A * d}$$

Where *m* is the mass of the particulate element (corrected using average of all blanks) to the total cannister volume (6.2 L), *A* is the area of the cannister opening (0.012 m^2) and *d* is the duration (days) the trap was drifting. POC and PON samples were then corrected using blanks.

Faecal pellet and egg abundance and size

Faecal pellet (FP) samples were left to settle in the lab for > 48 hours. 200 ml of supernatant was carefully decanted off using a syringe. The remaining 50 ml was analysed under an Olympus SZX16 dissecting light microscope. Images of each sample were taken using a Canon EOS 60D DSLR camera, with size measurements subsequently analysed using ImageJ (Version 1.54g). FP were classified into three shapes, cylindrical, round (i.e. an almost sphere shape) and oval, with volume calculated using geometrical equations for a cylinder, sphere and oval respectively. FP abundance and total volume were normalised to total cannister volume and flux was calculated using Eq. 1. To estimate carbon content in cylindrical faecal pellets a conversion factor, derived from Antarctic samples, of 0.08 mg C mm^{-3} was used (Pauli et al., 2021).

Krill eggs were identified by size (~ 670 µm, George and Stromberg, 1985), with flux calculated and size estimated using the same method as faecal pellets. To estimate krill egg carbon, a conversion factor of 17.175 µg C per egg was calculated from Ikeda (1985) by averaging the carbon content (of embryos stage I-IV) and an average hatching success of 68.4% was applied, as only eggs which do not hatch contribute to the POC flux (Harrington and Ikeda, 1986).

Microplankton community abundance

A detailed description of collection and analysis methods are available in the supplementary (Supplementary Methods). In brief, microplankton samples were collected from the euphotic zone using a CTD and Niskin bottles and preserved with 5 mL acid Lugols' solution at 4 °C until analysis at Plymouth Marine Laboratory, Plymouth, UK. Samples were then concentrated through settling, and imaged using a FlowCam IV (Yokogawa Fluid Imaging Technologies). Subsequent images were processed using VisualSpreadsheet (v4.19.3), with particles classified to genus where possible (otherwise particles were assigned to broader taxonomic groups e.g. dinoflagellate, nanoflagellate etc). Ice associated phytoplankton taxa (commonly *Fragilariopsis* spp., *Entomoneis* spp., *Nitzschia* spp., *Cylindrotheca* spp. and large single centric diatoms) were subsequently compared with total protist abundance to evaluate their contribution to community structure.

Satellite imagery

Average sea ice extent was calculated as a median of daily sea ice concentration layers from the 4th to the 27th of February 2024, assuming threshold for an ice-covered pixel is 15% of its area using Advanced Microwave Scanning Radiometer-EOS 89-GHz channels (AMSR-E) (Spreen et al., 2008). Sea ice concentration data for individual sampling stations was generated as above selecting the values for the pixel corresponding to the geographic location of the sampling station. Bathymetry was compiled from the GEBCO bathymetric compilation group (GEBCO Bathymetric Compilation Group, 2025) with maps generated in ArcGIS Pro (version 3.6.0). Satellite images, including Sentinel-1 to 3 and Landsat-8 and 9, were downloaded from Google Earth Engine, taking into account the DST track geographical extent and deployment time. For the maps above the closest to the deployment time images were used. Subsequent images were prepared in QGIS (version 3.44).

https://doi.org/10.5194/egusphere-2026-988
Preprint. Discussion started: 27 February 2026

Results

Hydrological context

The DST was deployed in and amongst sea ice at stations S3 and S4 (Figure 2C, D). Though the rest of the stations have been classed as 'ice free', a substantial number of icebergs were present at S1 and S5, with S5 (Figure 2A, B, E) having been ice covered the previous day and S2 having been ice-covered two days prior (Supplementary table 1, Supplementary Figure 1, 2).

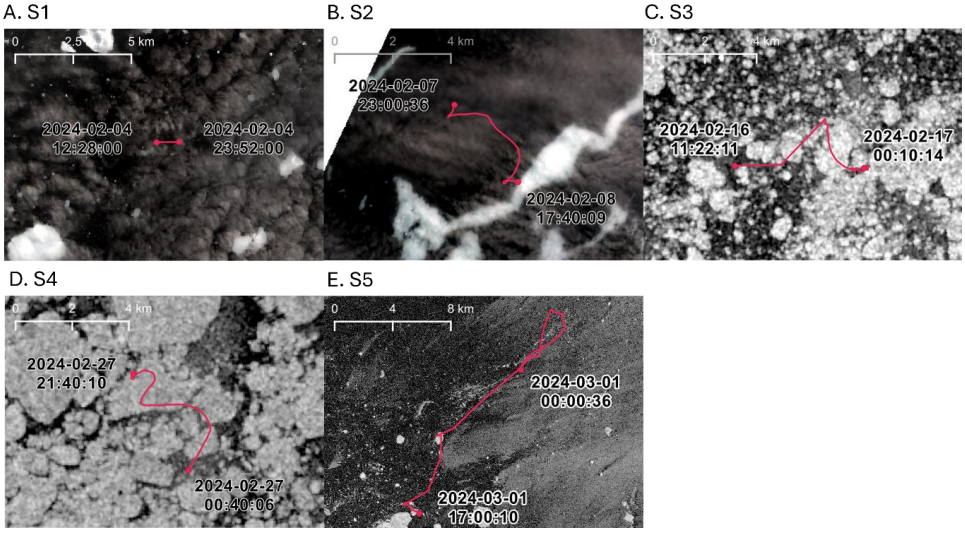

Figure 2 A-E. Satellite imagery with overlayed track data for the drifting sediment trap (Weddell Sea, February 2024). At S1 (A.) the drifting sediment trap was deployed next to the ship. Images produced by Mapping and Geographic Information Centre, British Antarctic Survey, 2025.

Temperature and salinity profiles of the top 150m of each station revealed the MLD ranged from 11-36 m (Figure 3, Supplementary table 1). Consequently, all flux measurements were taken below the MLD. S1 was the most productive station, with a chlorophyll peak of 0.88 µg L^{-1} at 8 m. In contrast S2 was the least productive station, with a chlorophyll maximum of 0.21 µg L^{-1} recorded at a considerable depth (89 m). The two 'ice stations', S3 and S4 had very low temperatures at the surface (-1.60 to -1.44 °C) and at depth (> 100 m, -1.76 to -1.59 °C). S4 had a warmer intrusion (maximum of -1.14 °C) at 16-34 m. All stations had fresher water at the surface, however this fresher layer was deepest at S2 and the two ice stations, S3 and S4.

https://doi.org/10.5194/egusphere-2026-988
Preprint. Discussion started: 27 February 2026

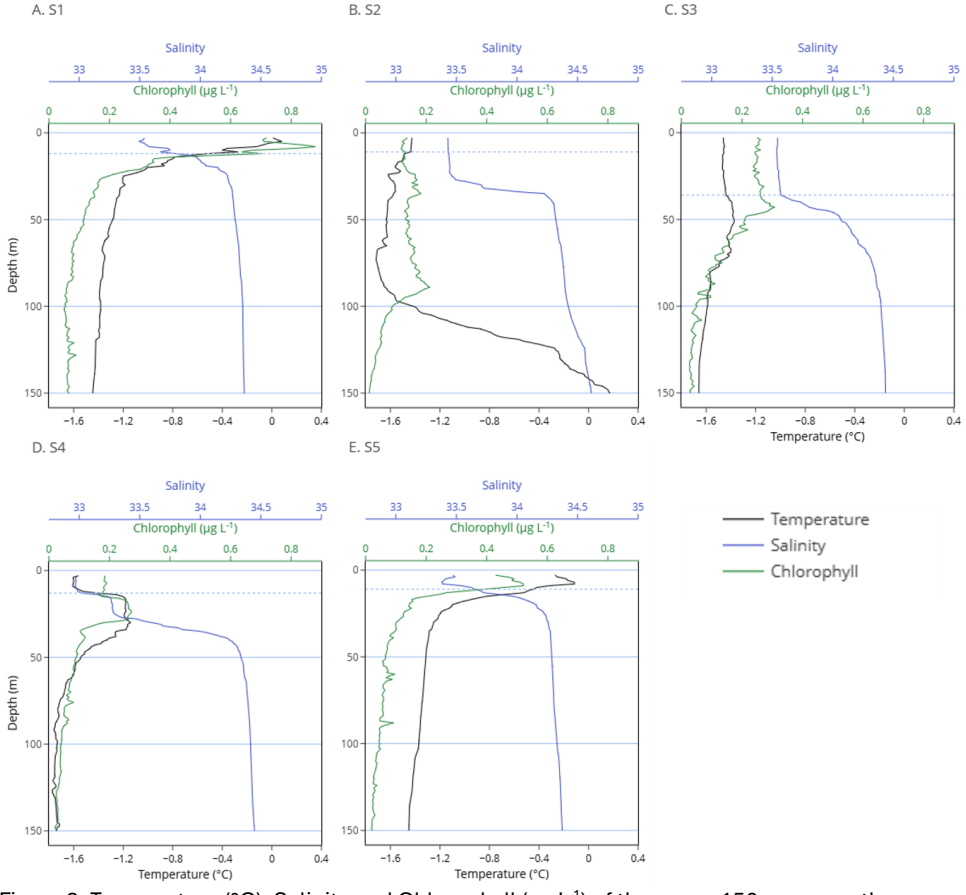

Figure 3. Temperature (°C), Salinity and Chlorophyll (µg L^{-1}) of the upper 150 m across the stations of the floating trap deployment (Weddell Sea, February 2024). Profiles were taken at deployment location with the exception of S4, which was the closest profile, taken 5 km from the deployment location (due to the presence of ice).

The Particulate Flux: Biogeochemical Composition

The greatest POC fluxes were observed at S1, wherein the POC flux increased with depth reaching a maximum of 364.1 mg C m^{-2} day^{-1} at 150 m depth (Figure 4 A). Higher POC fluxes were also observed at S3, however with an opposing trend, with a maximum of 220.0 mg C m^{-2} day^{-1} at 50 m, decreasing to 106.0 mg C m^{-2} day^{-1} at 150 m. S2, S4 and S5 had relatively uniform POC fluxes throughout all depths, with S5 showing a small increase at 100 m. S2 is the station with the lowest POC flux, averaging 51.3 mg C m^{-2} day^{-1} across all depths. Patterns in PON fluxes largely mirror the POC, with the highest PON fluxes at S1, and the lowest, and most uniform PON flux across all depths at S2 and S4 (Figure 4 B).

https://doi.org/10.5194/egusphere-2026-988
Preprint. Discussion started: 27 February 2026

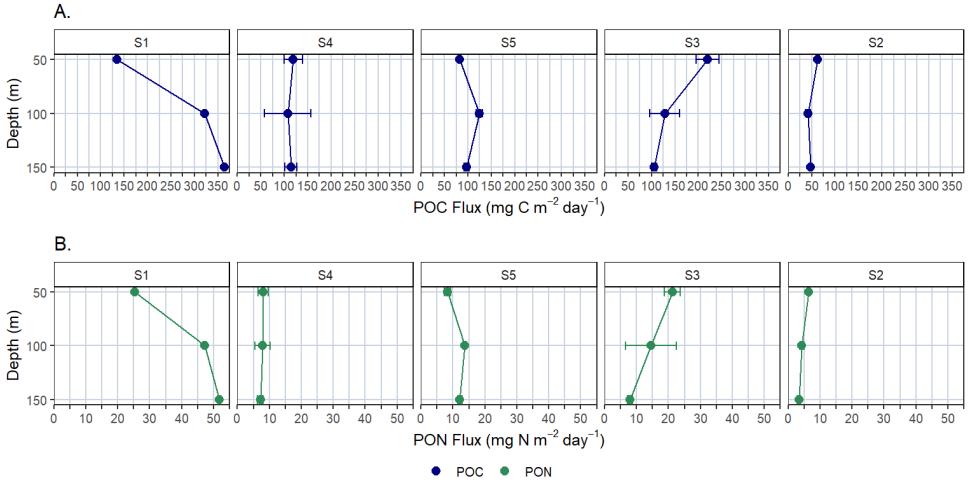

Figure 4. Mean vertical particulate flux (± standard deviation) observed at 50, 100, and 150 m across five deployments in the Weddell Sea (February 2024). A. particulate organic carbon flux, B. particulate organic nitrogen flux. Stations are numbered by sampling order, but the panel is arranged in a gradient from on shelf to off-shelf (left to right).

The POC:PON atomic ratios of sinking material tended to be substantially higher than Redfield (C:N, 6.63) (Redfield, 1934), with a median of 11.51 across all stations and depths. S1 had a POC:PON ratio closest to the Redfield ratio, followed by the S5 (Figure 5). S5 became more similar to Redfield at depth whereas S1 deviates from Redfield at the surface. The remaining stations (S2, S3, and S4) all had the largest POC:PON ratios at 150 m depth, with S4 having the highest average POC:PON ratio observed of 14.76.

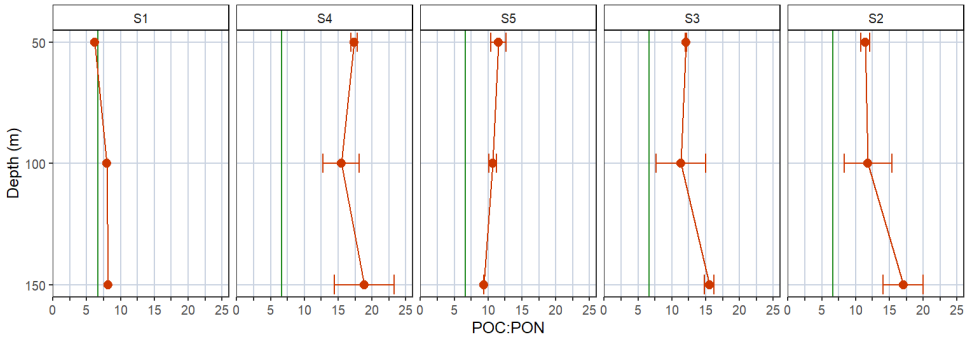

Figure 5. The mean POC:PON ratio (atomic, ± standard deviation) of the vertical particle flux at 50, 100 and 150 m across five deployments in the Weddell Sea (February 2024). The green line indicates the Redfield ratio of C:N (6.63). Stations are numbered by sampling order, but the panel is arranged in a gradient from on shelf to off-shelf (left to right).

The Particulate Flux: Faecal pellets and eggs.

https://doi.org/10.5194/egusphere-2026-988
Preprint. Discussion started: 27 February 2026

Across all stations and depths, the FP flux contributed a median of 47.9 % of the carbon flux (Figure 6 A). The faecal pellet flux was strongly driven by krill defecation, since cylindrical faecal pellets (FP) made up the overwhelming majority of pellets, representing 98% of the total FP volume flux (when summed across all stations and depths). Depth resolved patterns of FP contributions to the carbon flux did not mirror those of POC flux (Figure 4 A). However, stations with a higher POC flux generally had a greater FP flux (e.g. S1) and S2, with the lowest POC flux also has the lowest FP flux. S5 had the highest percentage of carbon represented by cylindrical FP, with a maximum of 99.0% at 150 m (Supplementary table 2). On the other hand, S2 and S4 had the lowest percentage carbon represented by FP, with both stations having minima at 50 m (S2, 17.4 % and S4, 25.8 %). Within each station, patterns in individual cylindrical FP volume (Figure 6 B.) were generally uniform across depth, with the exception of S1, where the median individual FP volume increased with depth.

S1 had the highest krill egg flux of 3990 eggs m^2 day^{-1} at 100 m and lowest krill egg flux of 1958 eggs m^2 day^{-1} at 150 m (Supplementary table 3). These eggs were estimated to represent between 2.9 – 6.7 % of total POC at their respective stations (Figure 7). S3 also had krill eggs present, estimated to represent 5.1 % of the total POC flux.

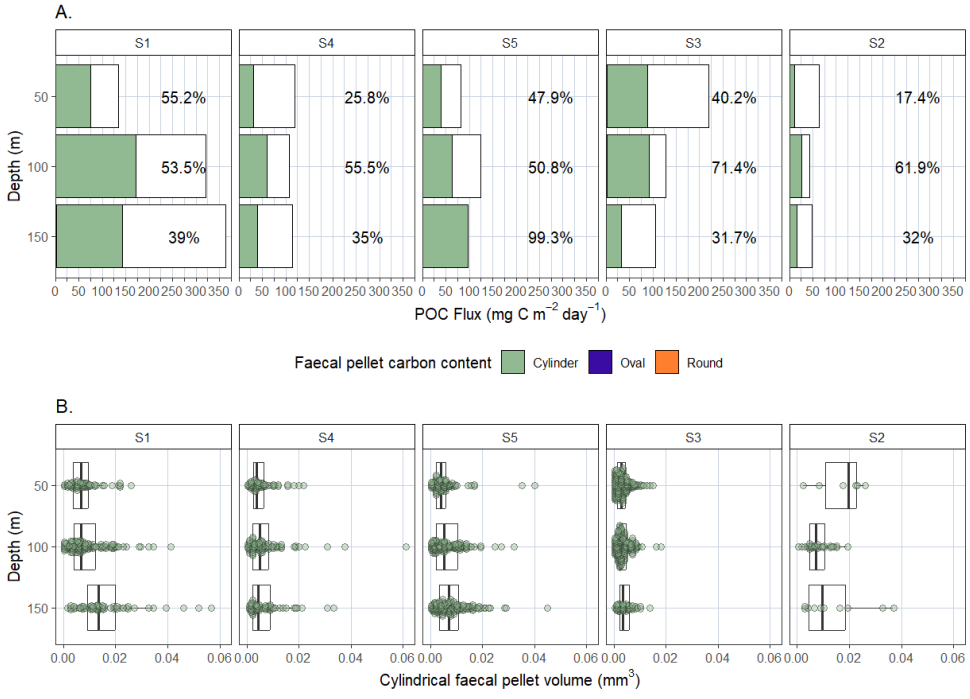

Figure 6 A. Estimated carbon content of all faecal pellets (green) as a proportion of the total POC flux (white) at each station. The estimated percentages of the total POC represented by faecal pellets are presented adjacent to each bar. B. Individual particle volumes of each cylindrical pellet identified. Throughout, stations are numbered by sampling order, but the panel is arranged in a gradient from on shelf to off-shelf (left to right).

https://doi.org/10.5194/egusphere-2026-988
Preprint. Discussion started: 27 February 2026

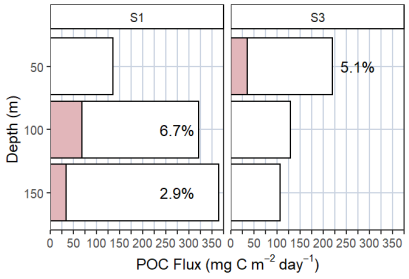

Figure 7. Estimated carbon content of Krill eggs (pink) compared with the mean total POC flux (white) in the Weddell Sea (February 2024) at stations where krill eggs were present. The estimated percentages of the total POC represented by krill eggs are presented adjacent to each bar

Discussion

The POC flux in the western Weddell Sea varied from 42.5 - 364.1mg C m^{-2} day^{-1} (mean of 123.2 mg C m^{-2} day^{-1}), with higher fluxes observed on the shelf (S1, S4, S3, S5) than off the shelf (S2). Despite its importance in global biogeochemical cycling and climate change disrupting sea ice production, contemporary direct particulate flux measurements in the Weddell Sea remain scarce (Joshi et al., 2024). Previous studies in the northern and eastern Weddell Sea have reported POC fluxes ranging from 24 to 112 mg C m^{-2} day^{-1} at depths of 150–250 m, with occasional extreme values exceeding 1000 mg C m^{-2} day^{-1} during spring bloom conditions (von Bodungen, 1986; Cadée, 1992; Dunbar, 1984; Isla et al., 2006; Wefer et al., 1990). The fluxes observed in our study fall well within this broad range, although the absence of extreme values likely reflects sampling late in the productive season (end of February), as the high values (> 1000 mg C m^{-2} day) reported by Cadée (1992) and von Bodungen et al., (1986) both occurred in spring (November/December). There are only a few observations of PON fluxes within the Weddell Sea. Thomas et al., (2001) and Michels et al., (2008) PON fluxes ranging from 0.51 - 20.86 mg N m^{-2} day^{-1} (10-230 m), which is the same order of magnitude as our observations (3.4 - 51.9 mg N m^{-2} day^{-1}).

The station closest to the coast (S1) had the highest chlorophyll concentration observed (0.88 µg L^{-1}, Figure 3), the highest POC and PON fluxes (Figure 4) and a mean POC:PON ratio of 7.45; close to the Redfield ratio of phytoplankton (6.63, Redfield, 1934). Together these values suggest high productivity and export with relatively fresh particulate material that has experienced little nitrogen remineralisation (Copin-Montegut and Copin-Montegut, 1983; Wakeham et al., 1997) (Figure 5). The higher POC fluxes observed across the shelf (S1, S3, S4, S5) likely reflects the higher concentrations of (micro)nutrients compared to the Weddell Sea open waters (Balaguer et al., 2023; Klunder et al., 2014; Middag et al., 2013). Moreover, the shallower water column of the shelf stations supports mixing and resuspension that facilitates nutrient resupply to the surface (Isla et al., 2006; Pudsey and King, 1997; Semper and Darelius, 2017).

Although the sea ice edge can also promote productivity there were no strong patterns observed in the particulate flux between sea ice and ice-free stations (Arrigo et al., 2008; Lannuzel et al., 2016; Smith and Nelson, 1985). This likely reflects the highly dynamic nature of sea ice during the sampling period. Stations were classified as ice-free based on

https://doi.org/10.5194/egusphere-2026-988
Preprint. Discussion started: 27 February 2026

conditions present during deployment, however, as the ice was constantly shifting, we suggest the particulate flux integrated longer term patterns in sea ice coverage which were minimised when we only accounted for deployment conditions. For instance, according to satellite images and coverage data, S2 (classed as 'ice free') was ice-covered two days prior to sampling (Supplementary figure 1, 2), and S5 had a variable sea ice coverage throughout February and January (Supplementary figure 3). The likelihood that most of our stations are heavily influenced by sea ice is supported also by patterns in POC:PON. With the exception of S1, the POC:PON ratio of the flux varies from 9.35 -18.84. This ratio exceeds both classic Redfield ratio for phytoplankton (6.63, Redfield, 1934) as well as the Southern Ocean specific ratio (mean of 6) (Tanioka et al., 2022). Particulate material commonly has a higher C:N relative to fresh phytoplankton (as nitrogen is preferentially absorbed by grazers and microbes with depth (Atkinson et al., 2012; Copin-Montegut and Copin-Montegut, 1983; Wakeham et al., 1997). For example, fresh Krill FP C:N has been shown to range between 3.2-13.2 (Atkinson et al., 2012; Manno et al., 2024). However, our range of ratios exceed values stated above, suggesting potential for the additional influence of ice associated biota across the stations which often have higher average C:N ratios, ranging from 6.2- 12.6 (Cozzi and Cantoni, 2011; Kennedy et al., 2002; Niemi and Michel, 2015). Indeed, phytoplankton community data from stations S2-S5 indicate that ice associated phytoplankton comprise and average 11.5-26.4% (mean of 18.2 %) of protists up to the 1% photosynthetically available radiance depth (Supplementary table 4). In addition, the mean contribution of ice associated algae at S1 is lower (7.7%), reflecting POC:PON patterns in our data. These findings highlight the limitations of categorising flux observations solely based on instantaneous ice conditions in dynamic polar environments.

Antarctic krill exerted a dominant control on the particulate carbon flux across shelf stations. Cylindrical faecal pellets, reliably identifiable as krill-derived, accounted for 98 % of total faecal pellet volume, and 88 % of cylindrical pellets were wider or equal to 80 µm, indicating they likely originated from *E. superba* (Atkinson et al., 2012). Using a conversion factor of 0.08 mg C mm^3 (Pauli et al., 2021), FP contributed between 17.4 and 99.0% of carbon to the total POC flux (with a median of 47.9 %), with the remaining carbon attributed to detritus (largely phytodetritus) (Figure 6 A). The carbon content of krill FP is not fixed, varying with grazing rates and food availability (Atkinson et al., 2012). Indeed, Pauli et al., (2021) reported a standard deviation of ±0.044 C mg mm^3 (equivalent to ± 55%), which could expand our estimated range of FP contribution to the POC flux, with the median value ranging between 26.3-74.2%. Despite this variability, stations with higher POC fluxes generally exhibited higher faecal pellet fluxes, indicating a strong coupling between krill activity and export magnitude. These observations reinforce previous findings that krill-mediated repackaging of organic matter into large, dense, fast-sinking particles is a key pathway for carbon export in the Southern Ocean (Belcher et al., 2017, 2019; Cavan et al., 2019; Manno et al., 2022; Trinh et al., 2023).

POC fluxes increased or remained relatively stable with depth across most stations (S1, S2, S4, S5) rather than attenuating rapidly. The absence of attenuation in our data may be explained by pulses of productivity in the recent past, lateral advection of material, or zooplankton interacting with and/or producing particulates at depth (e.g. Cavan et al., 2015; Freudenthal et al., 2001; Le Moigne et al., 2015; Smith et al., 2018). While temporal mismatches between production and collection cannot be fully excluded, physical processes such as lateral advection should have a minimal impact on 'catch efficiency' given the sediment trap was free drifting (Buesseler et al., 2000). We suggest instead that the consistent vertical patterns in faecal pellet flux are strongly indicative of zooplankton mediated control. Across most stations

https://doi.org/10.5194/egusphere-2026-988
Preprint. Discussion started: 27 February 2026

(S1-S4), krill faecal pellet flux peaked at 100 m, irrespective of surface chlorophyll concentration and environment. We propose this result is indicative of krill diel vertical migration (DVM), and production of pellets at depths between 50 and 100 m (below the MLD). Patterns in krill DVM are both highly variable and seasonal, although in summer krill often migrate to depths of up to 100 m (Bahlburg et al., 2023; Smith et al., 2025; Tarling et al., 2018), well reflecting the trends in our data. In addition, individual FP volumes remained largely consistent with depth across stations (Figure 6 B), suggesting that relatively little FP fragmentation took place between 50 and 150 m. As discussed above, this may support the hypothesis that krill are defecating at depth, meaning less opportunity for FP to fragment before they are collected at 100 or 150 m. Consistent FP volumes with depth may also reflect rapid sinking speeds and low fragmentation rates (either from higher particle integrity or minimal interaction with detritivores) (Atkinson et al., 2012; Briggs et al., 2020; Mayor et al., 2014). Regardless, this indicates that Krill FP have potential to strongly impact export as well as the upper ocean fluxes.

By producing faecal pellets below the mixed layer rather than at the surface, migrating krill effectively bypass near-surface remineralisation, enhancing the efficiency of carbon export (Liszka et al., 2019; Steinberg and Landry, 2017). Given estimated sinking rates of krill pellets (27–1218 m day^{-1}, mean of 309 m day^{-1}; Atkinson et al. 2012) a substantial fraction of this material could reach the seafloor on the shelf (average depth of 421m) within <1-15 days, contributing directly to benthic carbon supply and enhancing long-term sequestration. Carbon-specific krill pellet degradation rates have been estimated as a 23-30% loss at 300 m and up to a 35% loss at 500 m (Pauli et al., 2021; Wu et al., in review.). Consequently, across the shelf stations (S1, S3, S4, S5), between 19.8-111.2 mg C m^2 day^{-2} could reach the seafloor.

The contribution of krill to the particulate carbon flux was not limited to FPs. Krill eggs present at stations S1 and S3 potentially contributed (2.9-6.7 %) to the POC flux (Figure 7). The available food environment has a significant impact on maternal condition, egg quality and therefore hatching success (Quetin and Ross, 2001; Steinke et al., 2024; Yoshida et al., 2011). A substantial but undetermined fraction of these eggs will lead to deep carbon export, either through failure to hatch or through hatching to larvae which are non-viable or eaten while still at depth (Perry et al., 2020).Overall, our results highlight that krill eggs have the potential to contribute significantly to the particulate carbon flux, although their contribution is yet unquantified at an ocean scale.

Conclusions

This study provided observations of the particulate flux in the upper western Weddell Sea across multiple depths, a region of global importance for carbon sequestration and deep-water formation. We demonstrated that particulate fluxes in the upper 150 m are strongly structured by shelf processes, ice-associated production and zooplankton activity. POC and PON fluxes were higher on the shelf than open ocean, reflecting enhanced nutrient supply and biological productivity in shelf waters. In contrast, no clear distinction was found between sea ice and ice-free stations, reflecting the constant movement of the ice and that often our ‘ice free’ sites were still influenced by ice.

Krill exerted a strong control on the carbon flux across all shelf sites, with over 98 % of all FP belonging to krill, and contributions of up 99 % of the POC flux emphasising the role of zooplankton repackaging in mediating carbon export. The peak in FP flux occurred consistently at 100 m across the shelf, suggesting FP production at depth during krill daily vertical migration.

https://doi.org/10.5194/egusphere-2026-988
Preprint. Discussion started: 27 February 2026

Krill eggs are a poorly constrained component of the flux but our results highlight their potential role as a significant pathway for carbon transfer, particularly towards the end of the productive season where they may contribute up to 7 % of POC flux.

As climate change influences sea ice dynamics, the Southern Ocean is subject to dramatic change and it is unclear how zooplankton communities may react. Our finding show the importance of zooplankton mediated processes in driving carbon export within the upper 150 m, a region where particulate modification is most intense. Consequently, it is vital that biogeochemical studies in the euphotic zone, incorporate zooplankton processes (particularly diel vertical migration) to obtain a representative, process-based understanding of carbon cycling in a rapidly changing Southern Ocean.

Author contributions

FA prepared the original manuscript with contributions (review and editing) from all co-authors. FA collected data alongside ER, SF and KS, and conducted analysis with guidance from CM, CM contributed to conceptualisation of the project and equipment used with GF designing and building the custom equipment. EF analysed phytoplankton data and provided guidance on their interpretation. CM, AA, KS and SF contributed to funding acquisition.

Competing Interests

The authors declare that they have no conflict of interest

Financial support

This work was completed as part of the Processes Influencing Carbon Cycling: Observations of the Lower limb of the Antarctic Overturning (*PICCOLO*) project [NE/P021352/1 and NE/P021409/1].

Data availability

Data are available from the British Oceanographic data centre under the following DOIs 4A9FFBA99AB8E9BAE0637086ABC07E96, 4AA0669048E30212E0637086ABC0AF43

References

Alldredge, A. L. and Silver, M. W.: Characteristics, dynamics and significance of marine snow, Prog. Oceanogr., 20, 41–82, https://doi.org/10.1016/0079-6611(88)90053-5, 1988.

Arrigo, K. R., van Dijken, G. L., and Bushinsky, S.: Primary production in the Southern Ocean, 1997–2006, J. Geophys. Res. Oceans, 113, https://doi.org/10.1029/2007JC004551, 2008.

Atkinson, A., Schmidt, K., Fielding, S., Kawaguchi, S., and Geissler, P. A.: Variable food absorption by Antarctic krill: Relationships between diet, egestion rate and the composition and sinking rates of their fecal pellets, Deep Sea Research Part II: Topical Studies in Oceanography, 59–60, 147–158, https://doi.org/10.1016/j.dsr2.2011.06.008, 2012.

Atkinson, A., Hill, S. L., Pakhomov, E. A., Siegel, V., Anadon, R., Chiba, S., Daly, K. L., Downie, R., Fielding, S., Fretwell, P., Gerrish, L., Hosie, G. W., Jessopp, M. J., Kawaguchi, S., Krafft, B. A., Loeb, V., Nishikawa, J., Peat, H. J., Reiss, C. S., Ross, R. M., Quetin, L. B., Schmidt, K., Steinberg, D. K., Subramaniam, R. C., Tarling, G. A., and Ward, P.: KRILLBASE: a circumpolar database of Antarctic krill and salp numerical densities, 1926–2016, Earth Syst. Sci. Data, 9, 193–210, https://doi.org/10.5194/essd-9-193-2017, 2017.

https://doi.org/10.5194/egusphere-2026-988
Preprint. Discussion started: 27 February 2026

Bahlburg, D., Hüppe, L., Böhrer, T., Thorpe, S. E., Murphy, E. J., Berger, U., and Meyer, B.: Plasticity and seasonality of the vertical migration behaviour of Antarctic krill using acoustic data from fishing vessels, R. Soc. Open Sci., 10, https://doi.org/10.1098/rsos.230520, 2023.

Baker, C. A., Martin, A. P., Yool, A., and Popova, E.: Biological Carbon Pump Sequestration Efficiency in the North Atlantic: A Leaky or a Long-Term Sink?, Global Biogeochem. Cycles, 36, https://doi.org/10.1029/2021GB007286, 2022.

Balaguer, J., Koch, F., Flintrop, C. M., Völkner, C., Iversen, M. H., and Trimborn, S.: Iron and manganese availability drives primary production and carbon export in the Weddell Sea, Current Biology, 33, 4405-4414.e4, https://doi.org/10.1016/j.cub.2023.08.086, 2023.

Belcher, A., Tarling, G. A., Manno, C., Atkinson, A., Ward, P., Skaret, G., Fielding, S., Henson, S. A., and Sanders, R.: The potential role of Antarctic krill faecal pellets in efficient carbon export at the marginal ice zone of the South Orkney Islands in spring, Polar Biol., 40, 2001–2013, https://doi.org/10.1007/s00300-017-2118-z, 2017.

Belcher, A., Henson, S. A., Manno, C., Hill, S. L., Atkinson, A., Thorpe, S. E., Fretwell, P., Ireland, L., and Tarling, G. A.: Krill faecal pellets drive hidden pulses of particulate organic carbon in the marginal ice zone, Nat. Commun., 10, 889, https://doi.org/10.1038/s41467-019-08847-1, 2019.

von Bodungen, B.: Phytoplankton growth and krill grazing during spring in the Bransfield Strait, Antarctica — Implications from sediment trap collections, Polar Biol., 6, 153–160, https://doi.org/10.1007/BF00274878, 1986.

Brierley, A. S., Fernandes, P. G., Brandon, M. A., Armstrong, F., Millard, N. W., McPhail, S. D., Stevenson, P., Pebody, M., Perrett, J., Squires, M., Bone, D. G., and Griffiths, G.: Antarctic Krill Under Sea Ice: Elevated Abundance in a Narrow Band Just South of Ice Edge, Science (1979)., 295, 1890–1892, https://doi.org/10.1126/science.1068574, 2002.

Briggs, N., Dall'Olmo, G., and Claustre, H.: Major role of particle fragmentation in regulating biological sequestration of CO_2 by the oceans, Science (1979)., 367, 791–793, https://doi.org/10.1126/science.aay1790, 2020.

Brown, P. J., Jullion, L., Landschützer, P., Bakker, D. C. E., Naveira Garabato, A. C., Meredith, M. P., Torres-Valdés, S., Watson, A. J., Hoppema, M., Loose, B., Jones, E. M., Telszewski, M., Jones, S. D., and Wanninkhof, R.: Carbon dynamics of the Weddell Gyre, Southern Ocean, Global Biogeochem. Cycles, 29, 288–306, https://doi.org/10.1002/2014GB005006, 2015.

Buesseler, K. O., Steinberg, D. K., Michaels, A. F., Johnson, R. J., Andrews, J. E., Valdes, J. R., and Price, J. F.: A comparison of the quantity and composition of material caught in a neutrally buoyant versus surface-tethered sediment trap, Deep Sea Research Part I: Oceanographic Research Papers, 47, 277–294, https://doi.org/10.1016/S0967-0637(99)00056-4, 2000.

Buesseler, K. O., Boyd, P. W., Black, E. E., and Siegel, D. A.: Metrics that matter for assessing the ocean biological carbon pump, Proceedings of the National Academy of Sciences, 117, 9679–9687, https://doi.org/10.1073/pnas.1918114117, 2020.

Cadée, G. C.: Organic carbon in the upper layer and its sedimentation during the ice-retreat period in the Scotia-Weddell Sea, 1988, Polar Biol., 12, https://doi.org/10.1007/BF00238267, 1992.

https://doi.org/10.5194/egusphere-2026-988
Preprint. Discussion started: 27 February 2026

Carlson, C. A., Hansell, D. A., Peltzer, E. T., and Smith, W. O.: Stocks and dynamics of dissolved and particulate organic matter in the southern Ross Sea, Antarctica, Deep Sea Research Part II: Topical Studies in Oceanography, 47, 3201–3225, https://doi.org/10.1016/S0967-0645(00)00065-5, 2000.

Cavan, E. L., Le Moigne, F. A. C., Poulton, A. J., Tarling, G. A., Ward, P., Daniels, C. J., Fragoso, G. M., and Sanders, R. J.: Attenuation of particulate organic carbon flux in the Scotia Sea, Southern Ocean, is controlled by zooplankton fecal pellets, Geophys. Res. Lett., 42, 821–830, https://doi.org/10.1002/2014GL062744, 2015.

Cavan, E. L., Belcher, A., Atkinson, A., Hill, S. L., Kawaguchi, S., McCormack, S., Meyer, B., Nicol, S., Ratnarajah, L., Schmidt, K., Steinberg, D. K., Tarling, G. A., and Boyd, P. W.: The importance of Antarctic krill in biogeochemical cycles, Nat. Commun., 10, 4742, https://doi.org/10.1038/s41467-019-12668-7, 2019.

Copin-Montegut, C. and Copin-Montegut, G.: Stoichiometry of carbon, nitrogen, and phosphorus in marine particulate matter, Deep Sea Research Part A. Oceanographic Research Papers, 30, 31–46, https://doi.org/10.1016/0198-0149(83)90031-6, 1983.

Cozzi, S. and Cantoni, C.: Stable isotope (δ^{13}C and δ^{15}N) composition of particulate organic matter, nutrients and dissolved organic matter during spring ice retreat at Terra Nova Bay, Antarct. Sci., 23, 43–56, https://doi.org/10.1017/S0954102010000611, 2011.

Daly, K. L. and Macaulay, M. C.: Abundance and distribution of krill in the ice edge zone of the Weddell Sea, austral spring 1983, Deep Sea Research Part A. Oceanographic Research Papers, 35, 21–41, https://doi.org/10.1016/0198-0149(88)90055-6, 1988.

DeVries, T.: The Ocean Carbon Cycle, Annu. Rev. Environ. Resour., 47, 317–341, https://doi.org/10.1146/annurev-environ-120920-111307, 2022.

Dunbar, R. B.: Sediment trap experiments on the Antarctic continental margin, Antarct. J. US., 19.5, 70–71, 1984.

El-Sayed, S. Z. and Taguchi, S.: Primary production and standing crop of phytoplankton along the ice-edge in the Weddell Sea, Deep Sea Research Part A. Oceanographic Research Papers, 28, 1017–1032, https://doi.org/10.1016/0198-0149(81)90015-7, 1981.

Freudenthal, T., Neuer, S., Meggers, H., Davenport, R., and Wefer, G.: Influence of lateral particle advection and organic matter degradation on sediment accumulation and stable nitrogen isotope ratios along a productivity gradient in the Canary Islands region, Mar. Geol., 177, 93–109, https://doi.org/10.1016/S0025-3227(01)00126-8, 2001.

George, R. Y. and Stromberg, J.-O.: Development of eggs of Antarctic krill *Euphausia superba* in relation to pressure, Polar Biol., 4, 125–133, https://doi.org/10.1007/BF00263875, 1985.

Guihen, D., Fielding, S., Murphy, E. J., Heywood, K. J., and Griffiths, G.: An assessment of the use of ocean gliders to undertake acoustic measurements of zooplankton: the distribution and density of Antarctic krill (*Euphausia superba*) in the Weddell Sea., Limnol. Oceanogr. Methods, 12, 373–389, https://doi.org/10.4319/lom.2014.12.373, 2014.

Harrington, S. A. and Ikeda, T.: Laboratory observations on spawning, brood size and egg hatchability of the Antarctic krill *Euphausia superba* from Prydz Bay, Antarctica, Mar. Biol., 92, 231–235, https://doi.org/10.1007/BF00392840, 1986.

https://doi.org/10.5194/egusphere-2026-988
Preprint. Discussion started: 27 February 2026

Hoppema, M.: Weddell Sea is a globally significant contributor to deep-sea sequestration of natural carbon dioxide, Deep Sea Research Part I: Oceanographic Research Papers, 51, 1169–1177, https://doi.org/10.1016/j.dsr.2004.02.011, 2004.

Ikeda, T.: Metabolic rate and elemental composition (C and N) of embryos and non-feeding early larval stages of antarctic krill (*Euphausia superba* Dana), J. Exp. Mar. Biol. Ecol., 90, 119–127, https://doi.org/10.1016/0022-0981(85)90114-5, 1985.

Isla, E., Gerdes, D., Palanques, A., Gili, J.-M., and Arntz, W.: Particle fluxes and tides near the continental ice edge on the eastern Weddell Sea shelf, Deep Sea Research Part II: Topical Studies in Oceanography, 53, 866–874, https://doi.org/10.1016/j.dsr2.2006.02.010, 2006.

Johnson, G. C.: Quantifying Antarctic Bottom Water and North Atlantic Deep Water volumes, J. Geophys. Res. Oceans, 113, https://doi.org/10.1029/2007JC004477, 2008.

Joshi, M., Mestas-Nuñez, A. M., Ackley, S. F., Arndt, S., Macdonald, G. J., and Haas, C.: Seasonal and Interannual Variations in Sea Ice Thickness in the Weddell Sea, Antarctica (2019–2022) Using ICESat-2, Remote Sens. (Basel)., 16, 3909, https://doi.org/10.3390/rs16203909, 2024.

Kennedy, H., Thomas, D., Kattner, G., Haas, C., and Dieckmann, G.: Particulate organic matter in Antarctic summer sea ice: concentration and stable isotopic composition, Mar. Ecol. Prog. Ser., 238, 1–13, https://doi.org/10.3354/meps238001, 2002.

Klunder, M. B., Laan, P., De Baar, H. J. W., Middag, R., Neven, I., and Van Ooijen, J.: Dissolved Fe across the Weddell Sea and Drake Passage: impact of DFe on nutrient uptake, Biogeosciences, 11, 651–669, https://doi.org/10.5194/bg-11-651-2014, 2014.

Lacour, L., Llort, J., Briggs, N., Strutton, P. G., and Boyd, P. W.: Seasonality of downward carbon export in the Pacific Southern Ocean revealed by multi-year robotic observations, Nat. Commun., 14, 1278, https://doi.org/10.1038/s41467-023-36954-7, 2023.

Lannuzel, D., Vancoppenolle, M., van der Merwe, P., de Jong, J., Meiners, K. M., Grotti, M., Nishioka, J., and Schoemann, V.: Iron in sea ice: Review and new insights, Elementa: Science of the Anthropocene, 4, https://doi.org/10.12952/journal.elementa.000130, 2016.

Liszka, C. M., Manno, C., Stowasser, G., Robinson, C., and Tarling, G. A.: Mesozooplankton Community Composition Controls Fecal Pellet Flux and Remineralization Depth in the Southern Ocean, Front. Mar. Sci., 6, https://doi.org/10.3389/fmars.2019.00230, 2019.

Manno, C., Stowasser, G., Enderlein, P., Fielding, S., and Tarling, G. A.: The contribution of zooplankton faecal pellets to deep-carbon transport in the Scotia Sea (Southern Ocean), Biogeosciences, 12, 1955–1965, https://doi.org/10.5194/bg-12-1955-2015, 2015.

Manno, C., Fielding, S., Stowasser, G., Murphy, E. J., Thorpe, S. E., and Tarling, G. A.: Continuous moulting by Antarctic krill drives major pulses of carbon export in the north Scotia Sea, Southern Ocean, Nat. Commun., 11, 6051, https://doi.org/10.1038/s41467-020-19956-7, 2020.

Manno, C., Stowasser, G., Fielding, S., Apeland, B., and Tarling, G. A.: Deep carbon export peaks are driven by different biological pathways during the extended Scotia Sea (Southern Ocean) bloom, Deep. Sea. Res. 2 Top. Stud. Oceanogr., 205, https://doi.org/10.1016/j.dsr2.2022.105183, 2022.

Manno, C., Corsi, I., Rowlands, E., and Bergami, E.: Plastics counteract the ability of Antarctic krill to promote the blue carbon pathway in the deep ocean, Mar. Pollut. Bull., 209, 117238, https://doi.org/10.1016/j.marpolbul.2024.117238, 2024.

https://doi.org/10.5194/egusphere-2026-988
Preprint. Discussion started: 27 February 2026

564 Martin, J. H., Knauer, G. A., Karl, D. M., and Broenkow, W. W.: VERTEX: carbon cycling in the northeast
565 Pacific, Deep Sea Research Part A. Oceanographic Research Papers, 34, 267–285,
566 https://doi.org/10.1016/0198-0149(87)90086-0, 1987.

567 Mayor, D. J., Sanders, R., Giering, S. L. C., and Anderson, T. R.: Microbial gardening in the ocean's
568 twilight zone: Detritivorous metazoans benefit from fragmenting, rather than ingesting, sinking
569 detritus, BioEssays, 36, 1132–1137, https://doi.org/10.1002/bies.201400100, 2014.

570 Michels, J., Dieckmann, G. S., Thomas, D. N., Schnack-Schiel, S. B., Krell, A., Assmy, P., Kennedy, H.,
571 Papadimitriou, S., and Cisewski, B.: Short-term biogenic particle flux under late spring sea ice in the
572 western Weddell Sea, Deep Sea Research Part II: Topical Studies in Oceanography, 55, 1024–1039,
573 https://doi.org/10.1016/j.dsr2.2007.12.019, 2008.

574 Middag, R., de Baar, H. J. W., Klunder, M. B., and Laan, P.: Fluxes of dissolved aluminum and
575 manganese to the Weddell Sea and indications for manganese co-limitation, Limnol. Oceanogr., 58,
576 287–300, https://doi.org/10.4319/lo.2013.58.1.0287, 2013.

577 Le Moigne, F. A. C.: Pathways of Organic Carbon Downward Transport by the Oceanic Biological
578 Carbon Pump, Front. Mar. Sci., 6, https://doi.org/10.3389/fmars.2019.00634, 2019.

579 Le Moigne, F. A. C., Poulton, A. J., Henson, S. A., Daniels, C. J., Fragoso, G. M., Mitchell, E., Richier, S.,
580 Russell, B. C., Smith, H. E. K., Tarling, G. A., Young, J. R., and Zubkov, M.: Carbon export efficiency and
581 phytoplankton community composition in the Atlantic sector of the Arctic Ocean, J. Geophys. Res.
582 Oceans, 120, 3896–3912, https://doi.org/10.1002/2015JC010700, 2015.

583 Niemi, A. and Michel, C.: Temporal and spatial variability in sea-ice carbon:nitrogen ratios on
584 Canadian Arctic shelves, Elementa: Science of the Anthropocene, 3,
585 https://doi.org/10.12952/journal.elementa.000078, 2015.

586 Nissen, C., Timmermann, R., Hoppema, M., Gürses, Ö., and Hauck, J.: Abruptly attenuated carbon
587 sequestration with Weddell Sea dense waters by 2100, Nat. Commun., 13, 3402,
588 https://doi.org/10.1038/s41467-022-30671-3, 2022.

589 Orsi, A. H., Johnson, G. C., and Bullister, J. L.: Circulation, mixing, and production of Antarctic Bottom
590 Water, Prog. Oceanogr., 43, 55–109, https://doi.org/10.1016/S0079-6611(99)00004-X, 1999.

591 Pauli, N.-C., Flintrop, C. M., Konrad, C., Pakhomov, E. A., Swoboda, S., Koch, F., Wang, X.-L., Zhang, J.-
592 C., Brierley, A. S., Bernasconi, M., Meyer, B., and Iversen, M. H.: Krill and salp faecal pellets contribute
593 equally to the carbon flux at the Antarctic Peninsula, Nat. Commun., 12, 7168,
594 https://doi.org/10.1038/s41467-021-27436-9, 2021.

595 Perry, F. A., Kawaguchi, S., Atkinson, A., Sailley, S. F., Tarling, G. A., Mayor, D. J., Lucas, C. H., King, R.,
596 and Cooper, A.: Temperature–Induced Hatch Failure and Nauplii Malformation in Antarctic Krill,
597 Front. Mar. Sci., 7, https://doi.org/10.3389/fmars.2020.00501, 2020.

598 Pudsey, C. J. and King, P.: Particle fluxes, benthic processes and the palaeoenvironmental record in
599 the Northern Weddell Sea, Deep Sea Research Part I: Oceanographic Research Papers, 44, 1841–
600 1876, https://doi.org/10.1016/S0967-0637(97)00064-2, 1997.

601 Quetin, L. B. and Ross, R. M.: Environmental Variability and Its Impact on the Reproductive Cycle of
602 Antarctic Krill, Am. Zool., 41, 74–89, https://doi.org/10.1093/icb/41.1.74, 2001.

https://doi.org/10.5194/egusphere-2026-988
Preprint. Discussion started: 27 February 2026

Redfield, A. C.: On the Proportions of Organic Derivatives in Sea Water and Their Relation to the Composition of Plankton, James Johnstone Memorial Volume, University Press of Liverpool, 176-192., 1934.

Rowlands, E., Bergami, E., Flint, G., Flores Ruiz, I., Hunter, A., Yang, S., Miserocchi, S., and Manno, C.: Missing microplastics in the Mediterranean (Adriatic) sea and their influence on deep carbon export, Under review.

Semper, S. and Darelius, E.: Seasonal resonance of diurnal coastal trapped waves in the southern Weddell Sea, Antarctica, Ocean Science, 13, 77–93, https://doi.org/10.5194/os-13-77-2017, 2017.

Smith, A. J. R., Wotherspoon, S., Ratnarajah, L., Cutter, G. R., Macaulay, G. J., Hutton, B., King, R., Kawaguchi, S., and Cox, M. J.: Antarctic krill vertical migrations modulate seasonal carbon export, Science (1979)., 387, https://doi.org/10.1126/science.adq5564, 2025.

Smith, K. L., Ruhl, H. A., Huffard, C. L., Messié, M., and Kahru, M.: Episodic organic carbon fluxes from surface ocean to abyssal depths during long-term monitoring in NE Pacific, Proceedings of the National Academy of Sciences, 115, 12235–12240, https://doi.org/10.1073/pnas.1814559115, 2018.

Smith, W. O. and Nelson, D. M.: Phytoplankton Bloom Produced by a Receding Ice Edge in the Ross Sea: Spatial Coherence with the Density Field, Science (1979)., 227, 163–166, https://doi.org/10.1126/science.227.4683.163, 1985.

Spreen, G., Kaleschke, L., and Heygster, G.: Sea ice remote sensing using AMSR-E 89-GHz channels, J. Geophys. Res. Oceans, 113, https://doi.org/10.1029/2005JC003384, 2008.

Steinberg, D. K. and Landry, M. R.: Zooplankton and the Ocean Carbon Cycle, Ann. Rev. Mar. Sci., 9, 413–444, https://doi.org/10.1146/annurev-marine-010814-015924, 2017.

Steinke, K. B., Bernard, K. S., Reiss, C. S., Walsh, J., Correa, G. M., and Stammerjohn, S. E.: Factors impacting the timing of reproductive development in female Antarctic krill at the northwestern Antarctic Peninsula, Front. Mar. Sci., 11, https://doi.org/10.3389/fmars.2024.1383175, 2024.

Tanioka, T., Garcia, C. A., Larkin, A. A., Garcia, N. S., Fagan, A. J., and Martiny, A. C.: Global patterns and predictors of C:N:P in marine ecosystems, Commun. Earth Environ., 3, 271, https://doi.org/10.1038/s43247-022-00603-6, 2022.

Tarling, G. A., Thorpe, S. E., Fielding, S., Klevjer, T., Ryabov, A., and Somerfield, P. J.: Varying depth and swarm dimensions of open-ocean Antarctic krill *Euphausia superba* Dana, 1850 (Euphausiacea) over diel cycles., Journal of Crustacean Biology, 38, 1–12, 2018.

Thomas, D., Kennedy, H., Kattner, G., Gerdes, D., Gough, C., and Dieckmann, G.: Biogeochemistry of platelet ice: its influence on particle flux under fast ice in the Weddell Sea, Antarctica, Polar Biol., 24, 486–496, https://doi.org/10.1007/s003000100243, 2001.

Trinh, R., Ducklow, H. W., Steinberg, D. K., and Fraser, W. R.: Krill body size drives particulate organic carbon export in West Antarctica, Nature, 618, 526–530, https://doi.org/10.1038/s41586-023-06041-4, 2023.

Turner, J. T.: Zooplankton fecal pellets, marine snow, phytodetritus and the ocean's biological pump, Prog. Oceanogr., 130, 205–248, https://doi.org/10.1016/j.pocean.2014.08.005, 2015.

Volk, T. and Hoffert, M. I.: The Carbon cycle and atmospheric CO_2: natural variations, Archean to present, edited by: Sundquist, E. T. and Broecker, W. S., American Geophysical Union, 627 pp., 1985.

https://doi.org/10.5194/egusphere-2026-988
Preprint. Discussion started: 27 February 2026

643 Wakeham, S. G., Lee, C., Hedges, J. I., Hernes, P. J., and Peterson, M. J.: Molecular indicators of
644 diagenetic status in marine organic matter, Geochim. Cosmochim. Acta, 61, 5363–5369,
645 https://doi.org/10.1016/S0016-7037(97)00312-8, 1997.

646 Wefer, G., Fischer, G., Fütterer, D. K., Gersonde, R., Honjo, S., and Ostermann, D.: Particle
647 Sedimentation and Productivity in Antarctic Waters of the Atlantic Sector, in: Geological History of
648 the Polar Oceans: Arctic versus Antarctic, Springer Netherlands, Dordrecht, 363–379,
649 https://doi.org/10.1007/978-94-009-2029-3_20, 1990.

650 Whitehouse, M., Atkinson, A., Ward, P., Korb, R., Rothery, P., and Fielding, S.: Role of krill versus
651 bottom-up factors in controlling phytoplankton biomass in the northern Antarctic waters of South
652 Georgia, Mar. Ecol. Prog. Ser., 393, 69–82, https://doi.org/10.3354/meps08288, 2009.

653 Wu, N., Hunter, A., and Manno C.: Microplastic-induced fragmentation reduces krill faecal-pellet
654 carbon export in the Southern Ocean: Evidence from mechanistic modelling., Under Review.

655 Yoshida, T., Virtue, P., Kawaguchi, S., and Nichols, P. D.: Factors determining the hatching success of
656 Antarctic krill *Euphausia superba* embryo: lipid and fatty acid composition, Mar. Biol., 158, 2313–
657 2325, https://doi.org/10.1007/s00227-011-1735-2, 2011.

658